

# **Hydrothermally Engineered Ni-CuC Hybrid nanocomposites: Structural and Morphological Investigations with Potential Fuel Catalytic Applications**

Sana Rasheed<sup>1,2</sup>, Farooq Sher<sup>3,\*</sup>, Tahir Rasheed<sup>4,\*</sup>, Saba Sehar<sup>1,2</sup>, Mansour Al Qubeissi<sup>3</sup>, Fatima Zafar<sup>2,5</sup>, Eder C. Lima<sup>6</sup>

<sup>1</sup>*Department of Chemistry, University of Agriculture, Faisalabad 38040, Pakistan*

<sup>2</sup>*International Society of Engineering Science and Technology, Coventry, United Kingdom*

<sup>3</sup>*School of Mechanical, Aerospace and Automotive Engineering, Faculty of Engineering, Environmental and Computing, Coventry University, Coventry CV1 5FB, United Kingdom*

<sup>4</sup>*School of Chemistry and Chemical Engineering, Shanghai Jiao Tong University, Shanghai, 200240, China*

<sup>5</sup>*Institute of Biochemistry and Biotechnology, University of the Punjab, Lahore 54590, Pakistan*

<sup>6</sup>*Institute of Chemistry, Federal University of Rio Grande do Sul (UFRGS), Av. Bento Goncalves 9500, P.O. Box 15003, ZIP 91501-970, Porto Alegre, RS, Brazil*

\*Corresponding author:

Dr. F. Sher

Assistant Professor

Department of Engineering, School of Science and Technology

Nottingham Trent University

Nottingham

NG11 8NS

UK

E-mail address: [Farooq.Sher@ntu.ac.uk](mailto:Farooq.Sher@ntu.ac.uk)

Tel.: +44 (0) 115 84 86679

## Abstract

Increasing travel demand, incomplete combustion of fuel in an engine, vehicle exhaust emissions such as NO<sub>x</sub>, CO and particulate matter and global warming urge the fuel modification methods by using nano additives and alternative fuel. Suitable preparation method, characterization and fuel additive application of nickel-copper-carbide nanocomposite (Ni-CuC NC) have been rarely reported due to lack of research. On this ground, the present research illustrated the synthesis of nickel-copper bimetallic nanoparticles (Ni-Cu BNPs) with copper chloride (CuCl<sub>2</sub>) and nickel nitrate (Ni(NO<sub>3</sub>)<sub>2</sub>·6H<sub>2</sub>O) salt precursors in the presence of sodium hydroxide (NaOH). Followed by the reinforcement of calcium carbide (CaC<sub>2</sub>) with Ni-Cu BNPs to prepare Ni-CuC nanocomposite via hydrothermal approach. Structural composition and morphological analysis of the Ni-CuC nanocomposite was studied by XRD and SEM respectively. Physical and combustion fuel properties were investigated at 20, 40, 60 and 80 ppm concentration of Ni-Cu BNPs and Ni-CuC nanocomposite respectively for fuel-efficiency. Flash and fire point of diesel fuel in the absence of additives was observed as 78 and 82 °C respectively. Whereas, 80 ppm fuel blend of Ni-CuC and Ni-Cu show a remarkable decrease in flash point up to 69 and 72 °C respectively. The decreasing trend for fire point observed up to 72 and 74 °C. A tremendous recorded decrease in kinematic viscosity was 1.51 and 1.75 m<sup>2</sup>/s with Ni-CuC and Ni-Cu. Ni-Cu BNPs and Ni-CuC nanocomposite in term of fuel efficiency and environment friendly emission could be recognized as potential candidates in diesel. Future work on Ni-Cu BNPs and Ni-CuC nanocomposite as fuel additives for enhancing fuel or biofuel parameters as a photocatalyst for various dye removal in wastewater treatment, as sensing agent in sensing technology as well as for chemical reaction catalysis could be encouraged.

**Keywords:** Hybrid nanocomposites; Bimetallic nanoparticles; Catalysis; Fuel additive; Crystal structure and Physio-chemical parameters.

## 1. Introduction

Fuel energy is the main operator of industrialization and the automotive industry all across the world. Conventional diesel fuel is the main energy supplier for the movement of goods and heavy equipments globally. Depletion of crude oil resources, rapid urbanization, individual mobility, increase energy demands, incomplete combustion of fuel and an elevated threat of global warming are major concerns throughout the world [1]. Combustion of fuel hydrocarbons gives energy as well as increases the emission of pollutants such as carbon monoxide, nitrogen dioxide (NO<sub>x</sub>), nitric oxide (N<sub>2</sub>O), volatile organic compounds (VOCs), and hydrocarbons (HCs). These pollutants cause the formation of smog, acidic rains, depletion of the ozone layer, increase of greenhouse phenomena and unwanted climatic changes [2]. Moreover, moving parts of the engine generate friction due to which around 10–15% of fuel energy is wasted and lowered the engine efficiency.

Innovative NPs and nanocomposites are being investigated via nanotechnology to enhance the Physico-chemical properties of the fuel and reduce exhaust emission such as NO<sub>x</sub> and CO gases [3-5]. Physico-chemical properties of fuel influence fuel engine performance and quality to a greater extent. Enhanced combustion and physical properties of fuel can be achievable with transition metal (Cu, Ni, Co, Cr, Pt, Zn) based NPs and nanocomposites [6-8]. Transition metals are used in the fabrication of NPs or nano-composites because of their abundance in nature as well as they are more economical and cheap [9]. In addition, transition metal such as Ni and Cu exhibit the resembling electronic structure with Pt and are used as alternative catalysts in chemical reactions [10-12].

The major drawbacks lie with the use of Ni and Cu metals are their low mechanical properties such as high ductility, low wear resistance and thermodynamically instability at elevated temperatures. In order to overcome the poor mechanical properties of transition metals, non-oxides such as carbides, nitrides, sulfides should be reinforced with these metals matrix [13]. Carbides, nitrides, sulfides show significant properties such as high melting point, corrosion resistance, high mechanical strength and high stability. They exhibit applications in refractory ceramics, catalysis, sensing technology, electrochemistry, wastewater management and fuel engine performances [14-17]. Transition metals (Ni, Cu, Co, Fe, Mn, Cr and Ti) with carbide show improved physico-chemical properties due to electron-rich bonding between metals and increase metal-metal (MM) bond spacing. As a result, the band contraction density of unoccupied d-orbitals decreases and leads to the DOS (density of states) around Fermi level and subsequent modified catalytic properties similar to those of noble metals [18, 19].

Researchers have analyzed the well-controlled morphology of nanocomposites by different methods such as wet sonochemical method, electrostatic spray deposition (ESD) and hydrothermal approach [20]. Among all, the hydrothermal approach has been used to attain specific diameter and longer stability of nanocomposite [21, 22]. Chaudary et al., [9] synthesized the Cu and Ni NPs with a simple chemical method and recorded their antimicrobial activity and found the sizes of 24 and 13 nm for Cu and Ni NPs with orthorhombic and monoclinic respective geometries. Cu and Ni NPs exhibit remarkable sensitivity at 100  $\mu\text{g/mL}$  against all tested micro-organisms. Guo et al., [23] fabricated the core-shell Ni-Cu NPs with modified tunable magnetic properties. It provides insight into the synthesis strategy of Cu–Ni core-shell nanocrystals with selectively exposed surfaces and morphologies. They studied the transformation shapes of Cu–Ni core-shell NPs from

cubes to tetra hexahedrons. Corn-like morphology or smooth surfaces were also acquired with core-shell nanowires.

An et al., [24] investigated the Cu-Ni NPs with Ni-rich surface for electrocatalytic methanol oxidation reaction (MOR). It reveals that the Ni-Cu alloy shows a mass current density of 1028 mA mg<sub>metal</sub><sup>-1</sup> for MOR at 1.55 V. At atomic level, redistribution of charges in the structure was promoted and Cu in Ni-Cu alloy contributed to hinder the formation of  $\gamma$ NiOOH (low-activity species). The Ni-Cu alloy catalyst shows significant long-term activity and stability for MOR and is considered to be an efficient non-precious metal catalyst. Carmona et al. [25] employed the Cu and Ni NPs in somatic cells of *Drosophila melanogaster* to study the genotoxic potential. Cu-NPs gone wrong to persuade mutant spots in the wings of fruit flies adults, demonstrated the absence of genotoxicity in somatic cells of *D. melanogaster*. However, no research has been conducted on Ni-Cu BNPs for fuel additive potential.

As far as is known, Ni-CuC NC have never been synthesized and used as a fuel nano additive. Therefore, in the present study, Ni-Cu BNPs and Ni-CuC nanocomposites were prepared with the assistance of the hydrothermal approach. The synthesized Ni-CuC nanocomposites were characterized by SEM and XRD for structural and morphological studies. Moreover, they are being employed as additives in diesel fuel to improve the efficiency of diesel by modifying its specific gravity, kinematic viscosity, flash point, fire point, cloud point, pour point and calorific values. Ni-CuC nanocomposites have a large number of empty vacancies on flat and small particle surfaces which make them adsorbed more aerial O<sub>2</sub> and fuel molecules on the nanocomposites. Thus, this phenomenon alters the physicochemical properties of fuel and provide better efficiency for engine fuel. Although numerous researches have been sought to investigate the formation of Ni-Cu BNPs and characterization. However, the effect of Ni-Cu BNPs and Ni-CuC nanocomposite

on diesel performance, combustion and emission characteristics have not been adequately discussed. The main purpose of this research is to find a suitable synthesis method for the preparation of Ni-Cu BNPs and Ni-CuC nanocomposite. Furthermore, the present work provides a comparative study of Ni-Cu BNPs and Ni-CuC nanocomposites as nano additives in the fuel to check the fuel efficiency.

## **2. Experimental**

### **2.1. Chemicals**

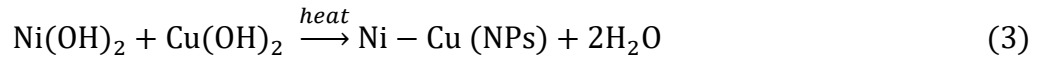
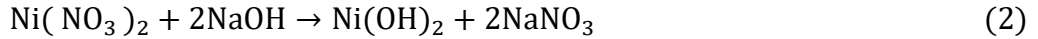
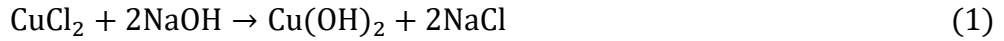
Hydrated salts of nickel such as nickel nitrate  $\text{Ni}(\text{NO}_3)_2 \cdot 6\text{H}_2\text{O}$ , copper chloride  $\text{CuCl}_2$ , urea  $\text{CO}(\text{NH}_2)_2$ , phenyl hydrazine ( $\text{C}_6\text{H}_8\text{N}_2$ ), calcium carbide ( $\text{CaC}_2$ ) and ethylene glycol ( $\text{C}_2\text{H}_6\text{O}_2$ ) were purchased from Sigma Aldrich. All the chemicals were used without further purification. The used chemicals were of analytical grade and de-ionised water (DI) was used to prepare all the solutions during the whole experimentation.

### **2.2. Synthesis of Ni-CuC nanocomposite**

Ni-Cu BNPs were prepared by a hydrothermal method which is given in

**Fig. 1.** For this, 0.6 g of  $\text{CuCl}_2$  and  $\text{Ni}(\text{NO}_3)_2 \cdot 6\text{H}_2\text{O}$  salts with an atomic ratio of 1:1 were dissolved in 60 mL of ethylene glycol. Then, stirred the mixture on a magnetic stirrer at 2400 rpm for 60 min to complete the mixing. In the next stage, 10 mL solution of NaOH (5 mol/L) as a surfactant was added dropwise into the solution and kept on stirring for 30 min. After that, phenyl hydrazine (10 mL) as a reducing agent was added into the solution and stirring of 60 min, turned the solution to dusty brown Ni-Cu precipitate with an oily layer. The solution was put into Teflon lined autoclave with 100 mL capacity and set the electric furnace at 180 °C temperature for 4 h. The reason for high temperature is that Ni cannot easily be reduced. After 4 h, the autoclave was cooled naturally

at room temperature and centrifuged the mixture at 4000 rpm with distilled water for 50 min. The process of centrifugation was repeated 2-3 times. Then, the sample was dried overnight at 60 °C and calcined at 600 °C for 6 h [26, 27] by following the hydrothermal reaction as shown in Eq. (1) to (3).



Following this, CaC<sub>2</sub> (0.15 g) was dissolved into ethylene glycol (60 mL) and stirred for 40 min. Eq. (4) illustrates the reduction of CaC<sub>2</sub> via ethylene glycol as a reducing agent during the hydrothermal method.



Then, 0.31 g of Ni-Cu BNPs were added into the chemically reduced solution of CaC<sub>2</sub> and stirred for 1 h which generate brown or black coloured Ni-CuC precipitates. For sample purification, put the sample into Teflon lined autoclave and placed into an electric furnace at 400 °C for 4 h. The sample was centrifuged at 4000 rpm with distilled water for 50 min and repeated the centrifugation 3–4 times. The sample was dried overnight at 60 °C and calcined at 600 °C for 6 h. [26, 27]. A schematic diagram of the fabrication method is shown in

**Fig. 1.** The prepared sample was geared up for further application.

### 2.3. Characterization

X-ray diffraction (XRD) pattern of synthesized Ni-CuC nanocomposites obtained on a Rigaku D/max Ultima III X-Ray diffractometer with a Cu-K<sub>α</sub> radiation source operated at 5 kV and 60 mA at a scanning step size of 0.030° and in 2θ range of 10–80°. SEM observations were performed

at 25 kV power and at 500×, 1000×, 2000× and 3000× resolutions which clearly describe the morphology of synthesized nanoparticles. For the calculation of the lattice parameter, the obtained results were analyzed with the use of MATCH software. To examine the flash point and fire point values throughout fuel additive application APEX-JCX309 Cleveland open cup tester was operated. APEX-JCX406 Bomb calorimeter at GB/T213 standard was used to achieve the calorimetric value of diesel fuel. The viscosity of 20, 40, 60 and 80 ppm solutions was investigated by using ASTM D445 Ostwald Viscometer. MPP 5Gs analyzer was used to compute the cloud and pour point [10, 26, 28, 29].

## 2.4. Diesel fuel additive

The properties of almost all the materials depend on their particle size. The large surface to volume ratio of small particles made them burn much more easily and have a short oxidizer diffusion length; enough energy was produced by oxidation to ignite and spontaneously combust. In general, metals have much more available energy as compared to conventional fuels per unit volume [30]. Physico-chemical parameters of diesel fuel were analyzed at a laboratory scale. The characterizations of all the properties were observed with the instigation of different concentrations ( $1.6 \times 10^{-3}$ –  $6.4 \times 10^{-3}$  g) of Ni-CuC nanocomposite and Ni-Cu BNPs in 80 mL of total diesel fuel. In order to prepare solutions of 20–80 ppm respective concentrations of nano additives and diesel fuel are given in **Table 1**. Combustion properties of diesel fuel were checked by calorific values, flash and fire point with the help of bomb calorimeter and Cleveland Open Cup Tester. Cleveland Open Cup has set off a temperature range from 10 to 350 °C. Similarly, physical properties such as kinematic viscosity, specific gravity, cloud point and pour point of diesel fuel comprising 20–80 ppm dosages of nano-additives were studied by Viscometer, Gravity meter and MPP 5Gs analyzer respectively [26, 29]. Then, the obtained results of flash point, fire point, cloud and pour



point, kinematic viscosity, calorific value and the specific gravity of Ni-Cu BNPs and Ni-CuC nanocomposite were compared and given as in **Table 2** and **Table 3**.

### **3. Results and discussion**

#### **3.1. X-ray diffraction and morphological identification**

The crystallographic structure of Ni-CuC NC is described through XRD pattern and specified in **Fig. 2**. XRD pattern provides the information on size and shape of unit cell from peak positions. The existence of strong peaks at 36.21, 43.54, 50.03 ° which are associated with (111), (202), (220) planes respectively indicating the presence of Cu with the space group Fm-3m [31]. While Ni shows three peaks at  $2\theta$  values of 38.52, 62.45, 68.78° with relative (200), (211), (310) planes respectively with the space group Fm-3m. Carbide shows sharp and strong peaks at  $2\theta$  values of 27.235° which is associated with (110) plane. The characteristic peak of Ni-CuC NC has high relative peak intensity (227) which is composed of two characteristic peaks of Ni (225) and Cu (225) indicates that Ni-CuC NC containing Ni and Cu BNPs. The strong and sharp diffraction peaks reveal the formation of a pure well crystalline structure of bimetallic Ni-CuC nanocomposite [32]. Furthermore, the XRD pattern exhibits no extra peak due to low noise. The characteristics of prepared spherical shaped Ni-CuC nanocomposites are clearly indicated by these sharp peaks associated with (110), (111), (220), (200) and (310) planes. Peak breadth specifies that the Ni-CuC nanocomposites are in the nanometer range and spherical in shape. By applying the Debye-Scherer formula as given in Eq. (6) to the XRD pattern of Ni-CuC nanocomposites, average crystalline size of NC is calculated as 29 nm.

$$D = 0.98\lambda / \beta \cos \theta \quad (6)$$

where  $D$  is the average crystallite size,  $\beta$  is the broadening of full width at half maximum (FWHM) intense peak,  $\theta$  is a Bragg's angle and  $\lambda$  is radiations wavelength [33]. The investigation of diffraction peaks demonstrated that Ni-CuC nanocomposites have a cubic crystal structure as shown in **Fig. 3**. Ni atoms bonded with Cu atoms in a fused-cluster manner because of 600 °C temperature during fabrication Carbide atoms are spread in the vacant interstitial sites of compactly packed Ni-Cu lattice. There are total 27 atoms in a one-unit cell as shown in **Fig. 3** with standard atomic colours. Unit cell exhibit the complex bonding arrangement in the dotted surface as shown in **Fig. 3(b-c)**. One unit cell possesses the thirteen polyhedral planes as shown in **Fig. 3(d)**. **Fig. 3(e-h)** shows the available lattice planes in Ni-CuC as (110), (111) and (211) respective planes. **Fig. 3(h)** represent the orientation of all available lattice planes in Ni-CuC as (110), (111) and (211) in one unit cell [4, 34].

The morphological study was followed by SEM analysis of Ni-CuC nanocomposites at 500, 1000, 2000, 3000× magnification after calcination at 600 °C and represented in **Fig. 4(a-d)**. **Fig. 4(a)** show small-sized Ni-Cu particles at 500× magnification. In **Fig. 4(b)** overall view of Ni-CuC show that particles tend to aggregate. The spherical shape particles are shown in **Fig. 4(c)** at 2000×. In **Fig. 4(d)** at 3000× the particles having a clear and smooth surface. SEM result revealed that Ni and Cu are homogeneously distributed over the entire surface of carbide particles with a very fine spherical structure and are well separated from each other [35].

## **3.2. Physico-chemical properties of fuel blends**

### **3.2.1. Effect of nano additives on flash point**

Effect of flash point at 20, 40, 60 and 80 ppm concentrations of Ni-CuC and Ni-Cu nano additives is shown in **Fig. 5**. Flash point of diesel fuel without nano-additives at 0 ppm shows a high temperature value of 78 °C. Linear trends indicated that flash point values of diesel fuel decreased

from 78 °C to 69 and 72 °C at 80 ppm concentration for Ni-CuC and Ni-Cu respectively. The decreasing trend of fire point values shows that Ni-CuC and Ni-Cu are efficient fuel catalysts having large surface area because of nanometer range which provide an enhanced number of active sites for reaction to occur. Hence Ni-CuC and Ni-Cu catalyst having attributes to increase the rate of fuel combustion which decrease ignition time of diesel fuel. This decreasing trend helps the vehicle's engine to start easily. Khan et al., [36] also examined the flash point of diesel fuel with CaSn<sub>3</sub> NPs as a fuel additive. CaSn<sub>3</sub> reduce the flash point up to 78 °C at 40 ppm. But the present study revealed that the Ni-CuC and Ni-Cu fuel blends show 70 and 75°C values for flash point. This is due to the reason that Ni-CuC and Ni-Cu have a limited tendency to reduce the flash point as compared to CaSn<sub>3</sub>. This limited decrease is associated with safe and reliable storage of diesel fuel.

### **3.2.2. Effect of nano additives on fire point**

At 0 ppm, fire point observed as 80 °C, which decreased up to 72 and 74 °C respectively with Ni-CuC and Ni-Cu at 80 ppm as given in **Fig. 6**. There is not much difference in these fire point values for fuel containing Ni-CuC and Ni-Cu nano additives. This decrease in fire point value indicates that Ni-CuC and Ni-Cu catalysts have a large surface to volume ratio and a higher number of vacant site on their surfaces. Uptake of O<sub>2</sub> from the air onto the vacancies enhances the rate of heat release and vaporization may help to reach the fire point earlier and start the engine without delay. Moreover, adsorbed O<sub>2</sub> react with toxic gases of diesel such as CO and SO and oxidized them into CO<sub>2</sub> and SO<sub>2</sub>. In this way, the Ni-CuC and Ni-Cu catalysts help to lower the pollutant emission threat in the environment. At 40 ppm Ni-CuC and Ni-Cu fuel blend show the fire point values like 75 and 80 °C. Jamil et al. [26] also investigated the fire point value with Co<sub>3</sub>O<sub>4</sub> fuel blend. It shows that Co<sub>3</sub>O<sub>4</sub> NPs fuel blend gives the fire point as 74 °C at 40 ppm concentration which is

comparable with the current result value. Thus, this trend also ensures fuel safety during storage with the addition of Ni-CuC and Ni-Cu nano additives.

### **3.2.3. Effect of nano additives on cloud point**

In the petroleum industry, cloud point of diesel fuel refers to the temperature at which wax in diesel starts to solidify [37]. It is illustrated in **Fig. 7** that the value of cloud point without nano additives is observed as  $-1\text{ }^{\circ}\text{C}$ . After the addition of Ni-CuC additive in fuel, cloud point decreases up to  $-7\text{ }^{\circ}\text{C}$  at 80 ppm. With the same concentration (80 ppm) of Ni-Cu fuel blend, cloud point decreases up to  $-5\text{ }^{\circ}\text{C}$  which means delayed wax crystallization formation in fuel in cold environmental conditions. Ni-CuC nano additives have weak intermolecular forces between atoms than metallic Ni-Cu catalyst consequently Ni-CuC show a much better effect on diesel's cloud point as compared to Ni-Cu. At 40 ppm, the cloud point of Ni-CuC fuel blend is  $-5\text{ }^{\circ}\text{C}$  and can be compared with already study of  $\text{CaSn}_3$  by Khan et al., [36]. Which stated that  $\text{CaSn}_3$  exhibit  $-6\text{ }^{\circ}\text{C}$  as cloud point at 40 ppm catalyst concentration. It is concluded that Ni-CuC shows good combustion abilities even at a low-temperature value of  $-7\text{ }^{\circ}\text{C}$ .

### **3.2.4. Effect of nano additives on pour point**

Pour point with 0–80 ppm concentrations of the Ni-CuC and Ni-Cu additive on diesel fuel exhibited the remarkable decrease in temperature from  $-3$  to  $-15\text{ }^{\circ}\text{C}$  and  $-3$  to  $-6\text{ }^{\circ}\text{C}$  respectively. **Fig. 8** shows that the decrease in the pour point is very slow with the addition of Ni-Cu as compared to the addition of Ni-CuC. Kalaimurugan et al., [38] also provided the insight of pour point of diesel and biodiesel for B20 and  $\text{Al}_2\text{O}_3$  blend which was  $-4\text{ }^{\circ}\text{C}$  at 25–100 ppm. These values are clearly higher than pour point values of Ni-CuC and Ni-Cu ( $-15$  and  $-6\text{ }^{\circ}\text{C}$ ) fuel blends used in the current study. In present research  $-15\text{ }^{\circ}\text{C}$  pour point temperature of Ni-CuC fuel blend indicated

that fuel will not freeze in engines at this temperature and will be utilized to inhibit fuel's freezing in cold regions.

### **3.2.5. Effect of nano additives on specific gravity**

The high specific gravity of Ni-CuC and Ni-Cu diesel fuel blends lower the rapid burning of fuel which decreases the fuel consumption and as a result, increase its life span. The influence of specific gravity on diesel fuel in the presence and absence of nano-additives is shown in **Fig. 9**. The specific gravity of Ni-CuC and Ni-Cu nano additive in diesel fuel was determined at 20, 40, 60 and 80 ppm concentration. Firstly, the specific gravity of the reference diesel solution (0 ppm) at room temperature was calculated which is about  $1.08 \text{ g/cm}^3$ . With a 40 ppm concentration of Ni-CuC nano-additive diesel fuel blend show the specific gravity of diesel increases up to  $1.13 \text{ g/cm}^3$ .

Specific gravity continuously increases up to  $1.15 \text{ g/cm}^3$  at the 80 ppm concentration as shown in **Fig. 9**. But in the case of Ni-Cu BNPs, the increasing trend of specific gravity approach only  $1.10 \text{ g/cm}^3$  value at 80 ppm. This show that Ni-Cu BNPs have not much influence on specific gravity as compared to Ni-CuC nanocomposites. In a previous study of  $\text{CoSn(OH)}_6$  NPs, Jamil et al., [39] reported the specific gravity to be  $0.79 \text{ g/cm}^3$  at 40 ppm. However, the current study gives specific gravity of Ni-CuC fuel blend as  $1.13 \text{ g/cm}^3$  at 40 ppm and act as a better fuel catalyst than  $\text{Co}_3\text{O}_4$  NPs. Therefore, provides better results in comparison to the previous study. The highest value of specific gravity with a high dosage of catalyst is due to the greater surface to volume ratio.

### **3.2.6. Effect of nano additives on kinematic viscosity**

Kinematic viscosity of diesel fuel was analyzed by the Ostwald viscometer at  $25 \text{ }^\circ\text{C}$  for 20–80 ppm sample of Ni-CuC and Ni-Cu nano-additive as illustrated in

**Fig. 10.** Kinematic viscosity of standard diesel at room temperature was calculated which is about 4.27 mm<sup>2</sup>/s in the absence of nano-additive. Kinematic viscosity decreases as the dosage of Ni-CuC and Ni-Cu nano-additive increases. The decrease in viscosity is attributed to the fact that nano additives release heat during mixing in fuel due to decreased attractive forces between fuel layers. Ni-CuC and Ni-Cu fuel blend at 40 ppm show kinematic viscosity values as 1.96 and 1.98 mm<sup>2</sup>/s respectively. As the dosage of additive increases in fuel, the amount of heat release boosted which contribute further to decrease the kinematic viscosity of the fuel.

On the other side, kinematic viscosity for Ni-CuC decreases up to 1.51 mm<sup>2</sup>/s which is also quite less than Ni-Cu (1.75 mm<sup>2</sup>/s) at 80 ppm concentration. While in the study of CaSn<sub>3</sub>, Khan et al., [36] analyzed the kinematic viscosity of fuel blend as 3.30 mm<sup>2</sup>/s at 40 ppm concentration. The lower kinematic viscosity trend of the present study indicates that the flowing resistance of fuel decreases with a high concentration of nano-additive due to the lower intermolecular interaction of fuel particles in the presence of the additive. The lower kinematic viscosity of diesel fuel is beneficial due to the fuel heating for appropriate atomization which supplies complete combustion and ignition. Moreover, during cold temperature, the low viscosity of diesel inhibits the freezing of fuel in the injector of the engine and protects the fuel filter and injectors from corrosion or wear [29].

### **3.2.7. Effect of nano additives on calorimetric values**

Calorific value is the amount of energy produced by the complete combustion of material or fuel [29]. Diesel fuel without additive exhibit a low calorific value of 930 J/g. 80 ppm concentrated solutions of Ni-CuC nanocomposites and Ni-Cu BNPs as a fuel additive in diesel enhances the calorific value up to 4 3,431 and 36,231 J/g respectively as shown in

**Fig. 11.** This indicates that as the concentration of catalyst increases, the calorific values also rise. With Ni-CuC nanocomposites addition in diesel fuel, better results are achieved as compared to Ni-Cu BNPs. An increase in the calorific value of diesel fuel indicates that the energy of fuel enhanced due to nano additives. On the other hand, calorific values for the  $\text{CoSn(OH)}_6$  [39] was observed as 31,412 J/g even at 80 ppm concentration. It can be clearly noticed that Ni-CuC nanocomposites and Ni-Cu BNPs show much better results as compared to  $\text{CoSn(OH)}_6$ . Metal nanocomposites and BNPs possesses high energy content than standard fuel and show a high surface area to volume ratio which contributes to the complete combustion of diesel fuel. Fuel combustion follows a superficial mechanism for nanocomposites and BNPs which is due to vacant sites in its crystal structure. Oxygen ( $\text{O}_2$ ) get adsorbed on vacant sites of crystal structure, which help the fuel molecules to burn completely in the presence of more oxygen availability. This phenomenon further facilitates the reduction of unburnt hydrocarbons in the exhaust of automobile [40].

#### **4. Conclusion**

Ni-CuC nanocomposites and Ni-Cu BNPs were successfully synthesized by the hydrothermal method which acted as efficient nano fuel additives. XRD analysis reveals that the Ni-CuC are pure, well crystalline and carbide particles are bonded to the Ni-Cu BNPs matrix. Carbide, Cu and Ni nanoparticles show sharp and strong peaks at  $2\theta$  values of 27.23, 36.21 and 38.52° associated with (110), (111), (200) planes respectively. Morphological characterization indicates that the particles of Ni-CuC nanocomposites are distinctively separate from each other and have a spherical shape with an average particle size of 29 nm. Physio-chemical properties of diesel such as flash point, fire point, cloud point, pour point and kinematic viscosity decreases up to 69, 72, -7, -10 °C and 1.51  $\text{mm}^2/\text{s}$  for 80 ppm solution of Ni-CuC nanocomposites. While for Ni-Cu BNPs, the

observing trend of flash point, fire point, cloud point, pour point and kinematic viscosity give 72, 74, -5, -6 °C and 1.75 mm<sup>2</sup>/s. Therefore, both nano additives increase the vaporization and flowing property of fuel. High specific gravity values of Ni-CuC fuel blend lower the fast burning of fuel which mean fuel consumption is reduced with enhanced life span. From all these experimental results, it is also clear that Ni-CuC nanocomposites have an efficient surface area and good catalytic properties as compared to Ni-Cu BNPs. However, Ni-Cu BNPs and Ni-CuC nanocomposites can improve the performance and combustion properties of diesel fuel and also reduce the exhaust emission when used in diesel. In the future, Ni-Cu BNPs and Ni-CuC nanocomposites as easy to fabricate and cost-efficient catalyst could be applicable at an industrial scale for other fuel additive applications.



## References

1. Mathew, J., J. Joy, and S.C. George, *Potential applications of nanotechnology in transportation: A review*. Journal of King Saud University-Science, 2019. **31**(4): p. 586-594.
2. Hassan, M.H.A., et al., *Kinetic and thermodynamic evaluation of effective combined promoters for CO<sub>2</sub> hydrate formation*. Journal of Natural Gas Science and Engineering, 2020: p. 103313.
3. Saxena, V., N. Kumar, and V.K. Saxena, *A comprehensive review on combustion and stability aspects of metal nanoparticles and its additive effect on diesel and biodiesel fuelled CI engine*. Renewable and Sustainable Energy Reviews, 2017. **70**: p. 563-588.
4. Zaleska-Medynska, A., et al., *Noble metal-based bimetallic nanoparticles: the effect of the structure on the optical, catalytic and photocatalytic properties*. Advances in colloid and interface science, 2016. **229**: p. 80-107.
5. Rasheed, T., et al., *Tailored functional polymeric vesicles as smart nanostructured materials for aqueous monitoring of transition metal cations*. Journal of Molecular Liquids, 2021. **327**: p. 114791.
6. El-Seesy, A.I., A.M. Attia, and H.M. El-Batsh, *The effect of Aluminum oxide nanoparticles addition with Jojoba methyl ester-diesel fuel blend on a diesel engine performance, combustion and emission characteristics*. Fuel, 2018. **224**: p. 147-166.
7. Pandey, A.K., et al., *The Effect of Cerium Oxide Nano Particles Fuel Additive on Performance and Emission of Karanja Biodiesel Fueled Compression Ignition Military 585kW Heavy Duty Diesel Engine*. 2018, SAE Technical Paper.
8. Sharma, G., et al., *A review on the advancement of nanoparticles and their composites: synthesis and applications*. J. King Saud Univ. Sci, 2017. **31**: p. 143-284.
9. Chaudhary, J., et al., *Synthesis and biological function of Nickel and Copper nanoparticles*. Heliyon, 2019. **5**(6): p. e01878.
10. Bayer, B.C., et al., *In situ observations of phase transitions in metastable nickel (carbide)/carbon nanocomposites*. The Journal of Physical Chemistry C, 2016. **120**(39): p. 22571-22584.
11. Kelly, T.G. and J.G. Chen, *Metal overlayer on metal carbide substrate: unique bimetallic properties for catalysis and electrocatalysis*. Chemical Society Reviews, 2012. **41**(24): p. 8021-8034.
12. Xiao, Y., J.-Y. Hwang, and Y.-K. Sun, *Transition metal carbide-based materials: synthesis and applications in electrochemical energy storage*. Journal of Materials Chemistry A, 2016. **4**(27): p. 10379-10393.
13. Rasheed, T., et al., *Photocatalytic and adsorptive remediation of hazardous environmental pollutants by hybrid nanocomposites*. Case Studies in Chemical and Environmental Engineering, 2020. **2**: p. 100037.
14. Korać, M., et al., *Advances in Thermochemical Synthesis and Characterization of the Prepared Copper/Alumina Nanocomposites*. Metals, 2020. **10**(6): p. 719.
15. Kuang, M., et al., *Interface engineering in transition metal carbides for electrocatalytic hydrogen generation and nitrogen fixation*. Materials Horizons, 2020. **7**(1): p. 32-53.
16. Ren, F., et al., *Preparation of Cu–Al<sub>2</sub>O<sub>3</sub> bulk nano-composites by combining Cu–Al alloy sheets internal oxidation with hot extrusion*. Journal of Alloys and Compounds, 2015. **633**: p. 323-328.
17. Sullivan, M.M., C.-J. Chen, and A. Bhan, *Catalytic deoxygenation on transition metal carbide catalysts*. Catalysis Science & Technology, 2016. **6**(3): p. 602-616.
18. Yan, Z., et al., *A bimetallic carbide Fe<sub>2</sub>MoC promoted Pd electrocatalyst with performance superior to Pt/C towards the oxygen reduction reaction in acidic media*. Applied Catalysis B: Environmental, 2015. **165**: p. 636-641.
19. Gao, Q., et al., *Metal non-oxide nanostructures developed from organic–inorganic hybrids and their catalytic application*. Nanoscale, 2014. **6**(23): p. 14106-14120.

20. Huang, D., et al., *Hydrothermal synthesis of  $M\text{Sn}(\text{OH})_6$  ( $M = \text{Co}, \text{Cu}, \text{Fe}, \text{Mg}, \text{Mn}, \text{Zn}$ ) and their photocatalytic activity for the destruction of gaseous benzene*. Chemical Engineering Journal, 2015. **269**: p. 168-179.
21. Wang, Z., et al., *Amorphous  $\text{CoSnO}_3@ \text{C}$  nanoboxes with superior lithium storage capability*. Energy & Environmental Science, 2013. **6**(1): p. 87-91.
22. Zhang, J., et al., *Synthesis of  $\text{Co}_2\text{SnO}_4$  hollow cubes encapsulated in graphene as high capacity anode materials for lithium-ion batteries*. Journal of Materials Chemistry A, 2014. **2**(8): p. 2728-2734.
23. Guo, H., et al., *Controllable synthesis of Cu–Ni core–shell nanoparticles and nanowires with tunable magnetic properties*. Chemical Communications, 2016. **52**(42): p. 6918-6921.
24. Yao, D., et al., *Graphene based copper-nickel bimetal nanocomposite: magnetically separable catalyst for reducing hexavalent chromium*. ChemistrySelect, 2020. **5**(11): p. 3243-3247.
25. Carmona, E.R., A. García-Rodríguez, and R. Marcos, *Genotoxicity of copper and nickel nanoparticles in somatic cells of *Drosophila melanogaster**. Journal of Toxicology, 2018. **2018**.
26. Jamil, S., M.R.S.A. Janjua, and S.R. Khan, *Synthesis and structural investigation of polyhedron  $\text{Co}_3\text{O}_4$  nanoparticles: Catalytic application and as fuel additive*. Materials Chemistry and Physics, 2018. **216**: p. 82-92.
27. Moumen, A., et al., *Nickel Colloid Nanoparticles: Synthesis, Characterization, and Magnetic Properties*. Journal of Cluster Science, 2019. **30**(3): p. 581-588.
28. Kang, J., et al., *In situ synthesis of nickel carbide-promoted nickel/carbon nanofibers nanocomposite catalysts for catalytic applications*. Chemical Engineering Journal, 2015. **275**: p. 36-44.
29. Sehar, S., et al., *Thermodynamic and kinetic study of synthesised graphene oxide-CuO nanocomposites: A way forward to fuel additive and photocatalytic potentials*. Journal of Molecular Liquids, 2020: p. 113494.
30. Hoseini, S., et al., *Performance and emission characteristics of a CI engine using graphene oxide (GO) nano-particles additives in biodiesel-diesel blends*. Renewable Energy, 2020. **145**: p. 458-465.
31. Nguyen, A.-M., et al., *Bimetallic Phosphide (Ni, Cu) 2P Nanoparticles by Inward Phosphorus Migration and Outward Copper Migration*. Chemistry of Materials, 2019. **31**(16): p. 6124-6134.
32. Long, X., et al., *Preparation, characterization and application in cobalt ion adsorption using nanoparticle films of hybrid copper–nickel hexacyanoferrate*. RSC Advances, 2019. **9**(13): p. 7485-7494.
33. Wang, J., et al., *One-Pot Synthesis of Dealloyed AuNi Nanodendrite as a Bifunctional Electrocatalyst for Oxygen Reduction and Borohydride Oxidation Reaction*. Advanced Functional Materials, 2017. **27**(23): p. 1700260.
34. Quaino, P., et al., *Understanding the structure and reactivity of NiCu nanoparticles: an atomistic model*. Physical Chemistry Chemical Physics, 2017. **19**(39): p. 26812-26820.
35. Sharma, G., et al., *Novel development of nanoparticles to bimetallic nanoparticles and their composites: a review*. Journal of King Saud University-Science, 2019. **31**(2): p. 257-269.
36. Khan, S.R., et al., *Template free synthesis of calcium-tin ( $\text{CaSn}_3$ ) bimetallic micro cubes: Characterization, catalytic activity, adsorption and additive properties*. Chemical Physics Letters, 2020. **739**: p. 136917.
37. Huang, G., et al., *Biodiesel production by microalgal biotechnology*. Applied energy, 2010. **87**(1): p. 38-46.
38. Kalaimurugan, K., et al., *Combustion analysis of  $\text{CuO}_2$  nanoparticles addition with neochloris oleoabundans algae biodiesel on CI engine*. Materials Today: Proceedings, 2020.
39. Jamil, S., et al., *First synthetic study of cube-like cobalt hydroxystannate nanoparticles as photocatalyst for Drimarene red K-4BL degradation and fuel additive*. Journal of Cluster Science, 2018. **29**(4): p. 685-696.

40. Khan, S.R., et al., *Agar and egg shell derived calcium carbonate and calcium hydroxide nanoparticles: Synthesis, characterization and applications*. Chemical Physics Letters, 2019. **732**: p. 136662.

## List of Tables

**Table 1.** Sample preparation for the measurement of physiochemical fuel properties.

<b>Concentration</b>	<b>Additive</b>	<b>Diesel</b>
<b>(ppm)</b>	<b>concentration</b>	<b>(mL)</b>
	<b>(g)</b>	
0	0	80
20	$1.6 \times 10^{-3}$	80
40	$3.2 \times 10^{-3}$	80
60	$4.8 \times 10^{-3}$	80
80	$6.4 \times 10^{-3}$	80

**Table 2.** Effect of Ni-CuC nano additive on physio-chemical properties of the fuel.

Parameters	Concentration of nano additives					References
	0 ppm	20 ppm	40 ppm	60 ppm	80 ppm	
Flash point (°C)	78	75	70	70	69	This work
	-	-	78	-	-	[36]
Fire point (°C)	82	80	75	74	72	This work
	64	68	74	-	-	[26]
Cloud point (°C)	-1	- 2	- 5	- 6	-7	This work
	-4	-5	-6	-	-	[36]
Pour point (°C)	-3	- 4	- 6	- 9	- 10	This work
	-4	-4	-4	-	-	[38]
Specific gravity (g/cm <sup>3</sup> )	1.08	1.12	1.13	1.14	1.15	This work
	0.79	-	0.79	0.79	0.79	[39]
Kinematic viscosity (mm <sup>2</sup> /s)	4.27	2.04	1.96	1.91	1.51	This work
	2.68	2.86	3.30	-	-	[36]
Calorific values (J/g)	930	12,704	30,817	41,342	43,431	This work
	920	-	12,604	20,819	31,412	[39]

**Table 3.** Effect of Ni-Cu nano additive on physio-chemical properties of fuel.

Parameters	Concentration of nano additives				
	0 ppm	20 ppm	40 ppm	60 ppm	80 ppm
Flash point (°C)	78	75	72	71	72
Fire point (°C)	82	81	80	76	74
Cloud point (°C)	-1	-3	-6	-5	-5
Pour point (°C)	-3	-5	-5	-7	-6
Specific gravity (g/cm <sup>3</sup> )	1.08	1.08	1.09	1.10	1.10
Kinematic viscosity (mm <sup>2</sup> /s)	4.27	2.03	1.98	1.95	1.75
Calorific values (J/g)	930	11,706	29,824	30,211	36,231

## List of Figures

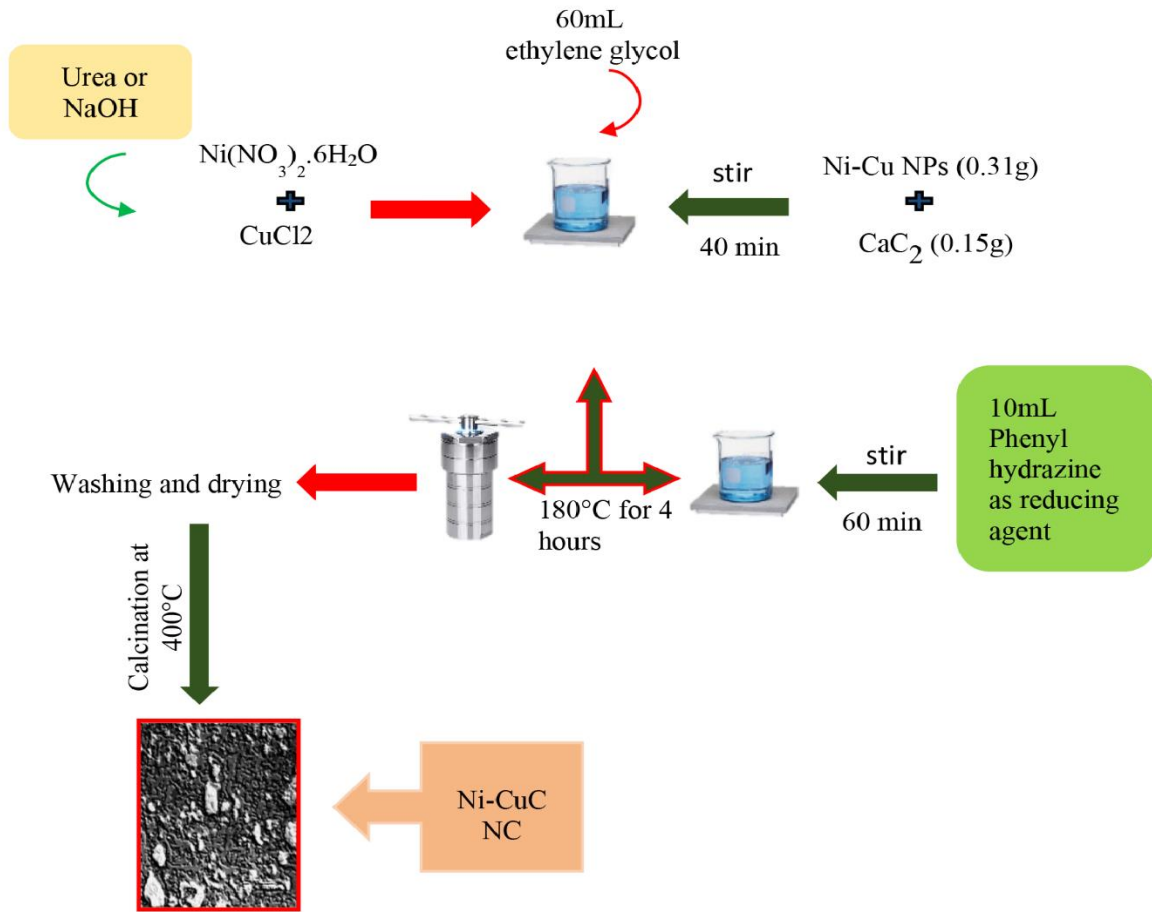


**Fig. 1.** Preparation scheme of Ni-Cu BNP and Ni-CuC nanocomposites.

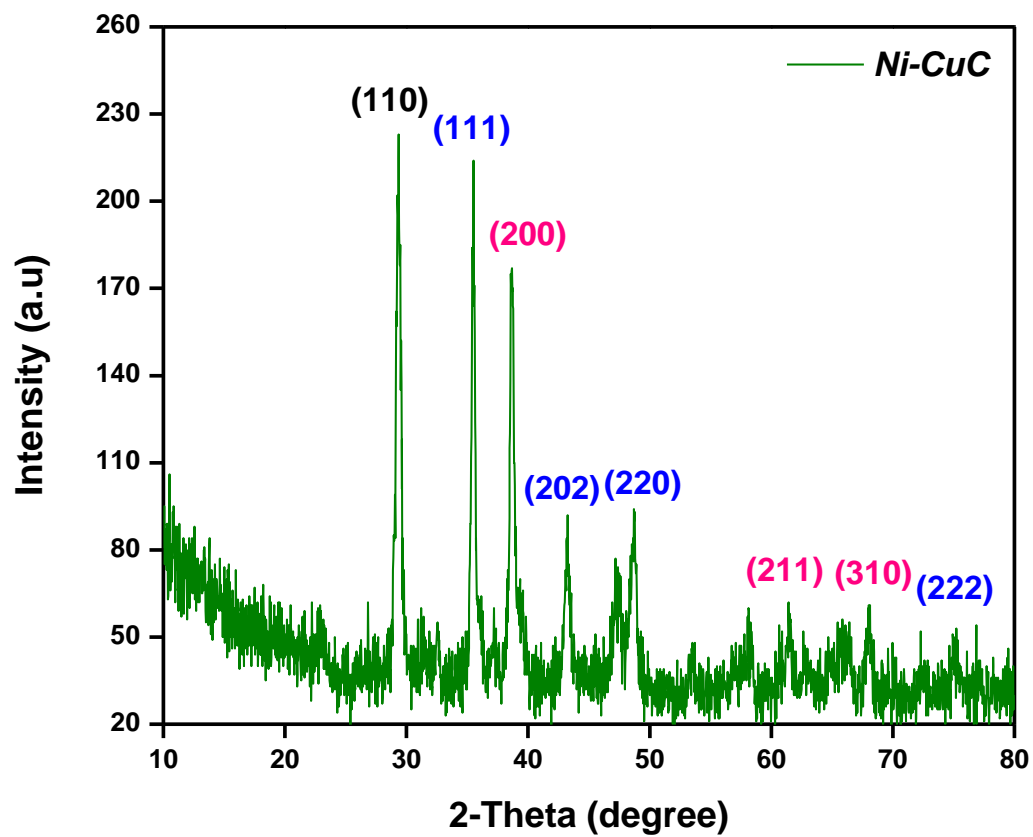


**Fig. 2.** XRD pattern of synthesized Ni-CuC nanocomposites.



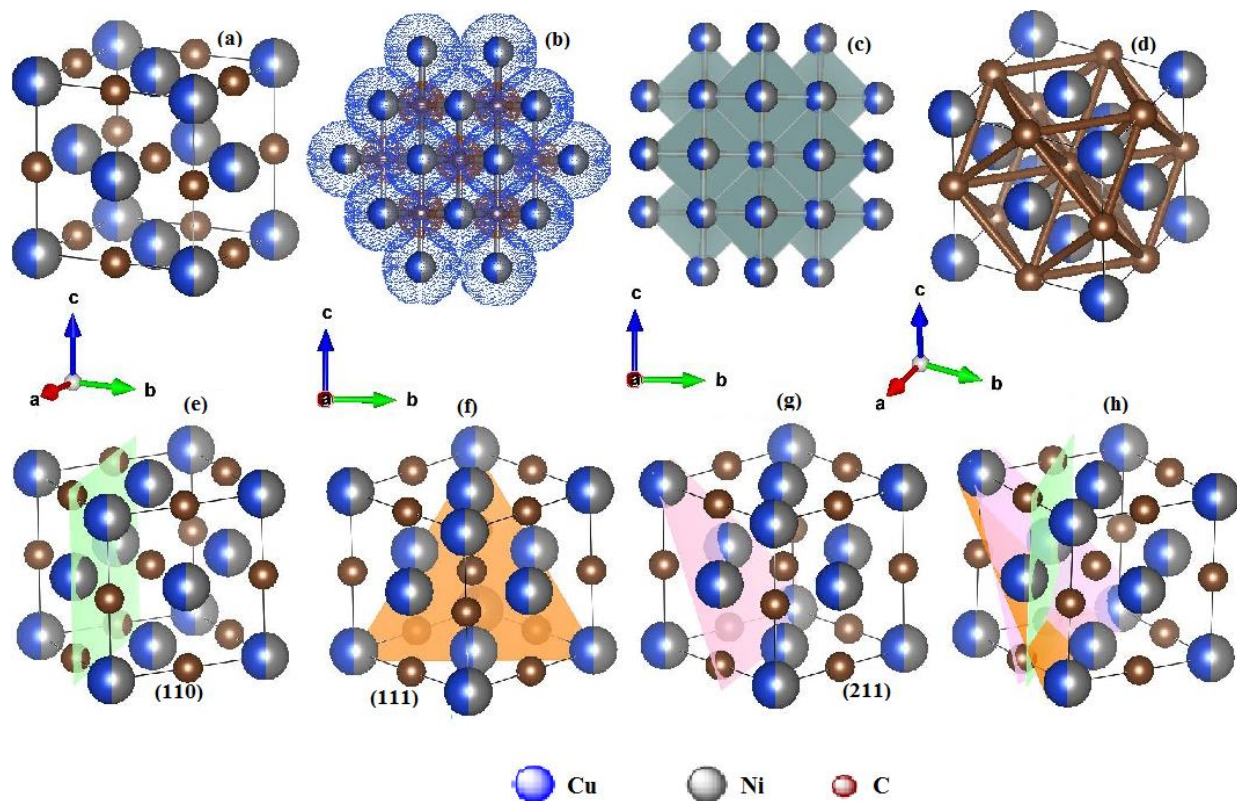


**Fig. 3.** Structural representation of (a) positions of Ni-Cu atoms bonded with C atoms in cubic unit cell, (b) dotted surface of unit cell atoms, (c) polyhedrons in unit cell, (d) Ni-Cu bonding with C at interstitial positions, (e) (110) plane, (f) (111) plane, (g) (211) plane and (h) all planes in one cubic unit cell at 3.51 Å from origin.

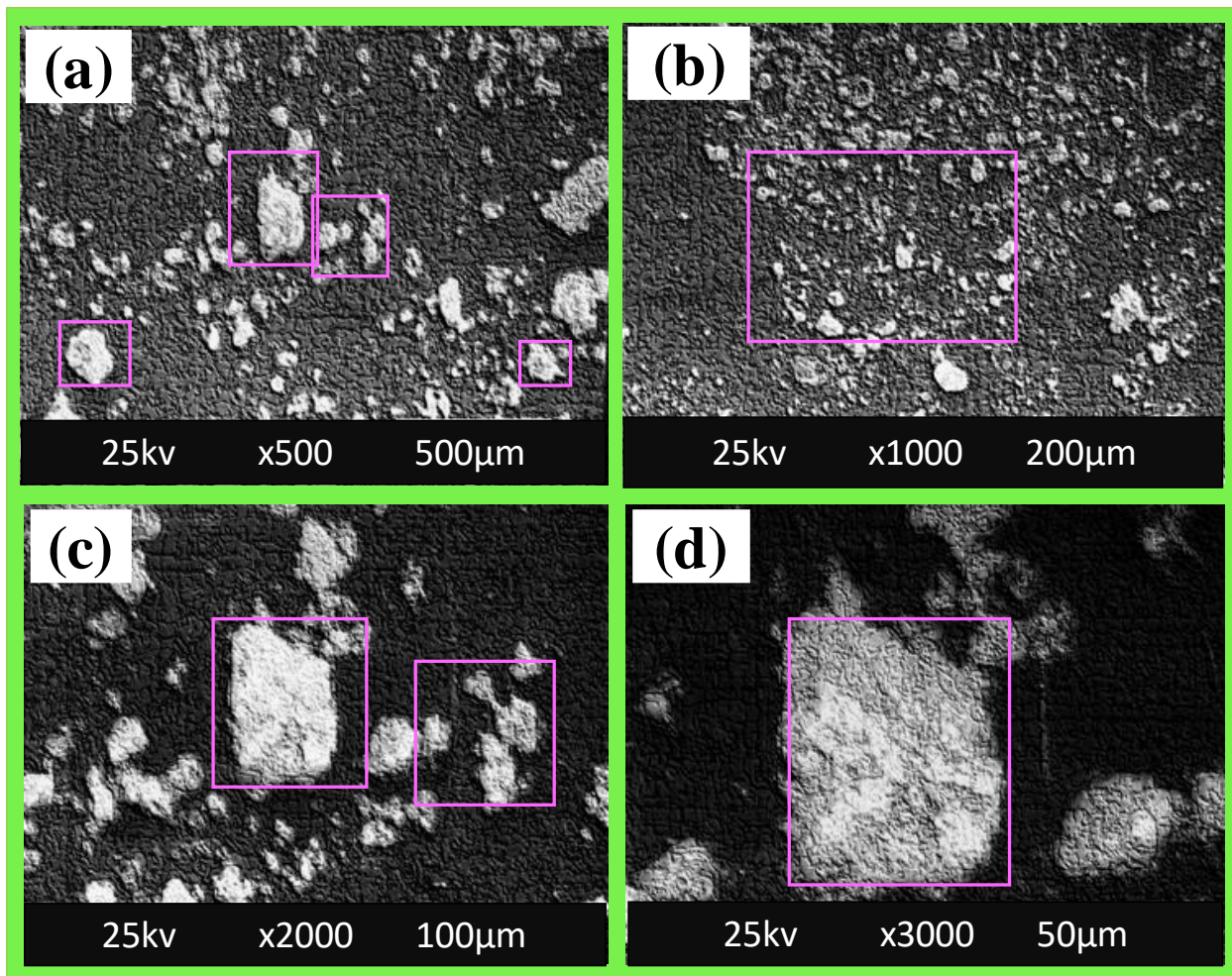


**Fig. 4.** SEM images of Ni-CuC nanocomposite at (a) 500× (b) 1000×, (c) 2000× and (d) 3000×.

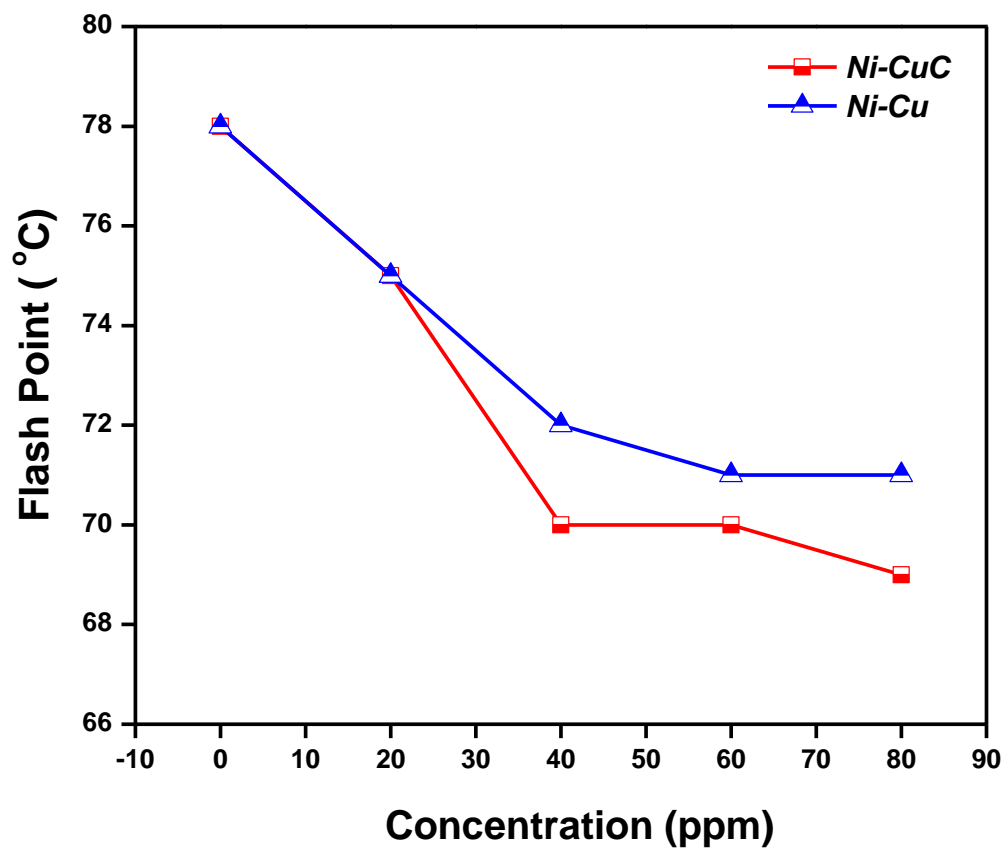


**Fig. 5.** Effect of Ni-Cu and Ni-CuC on the fuel flash point of diesel.

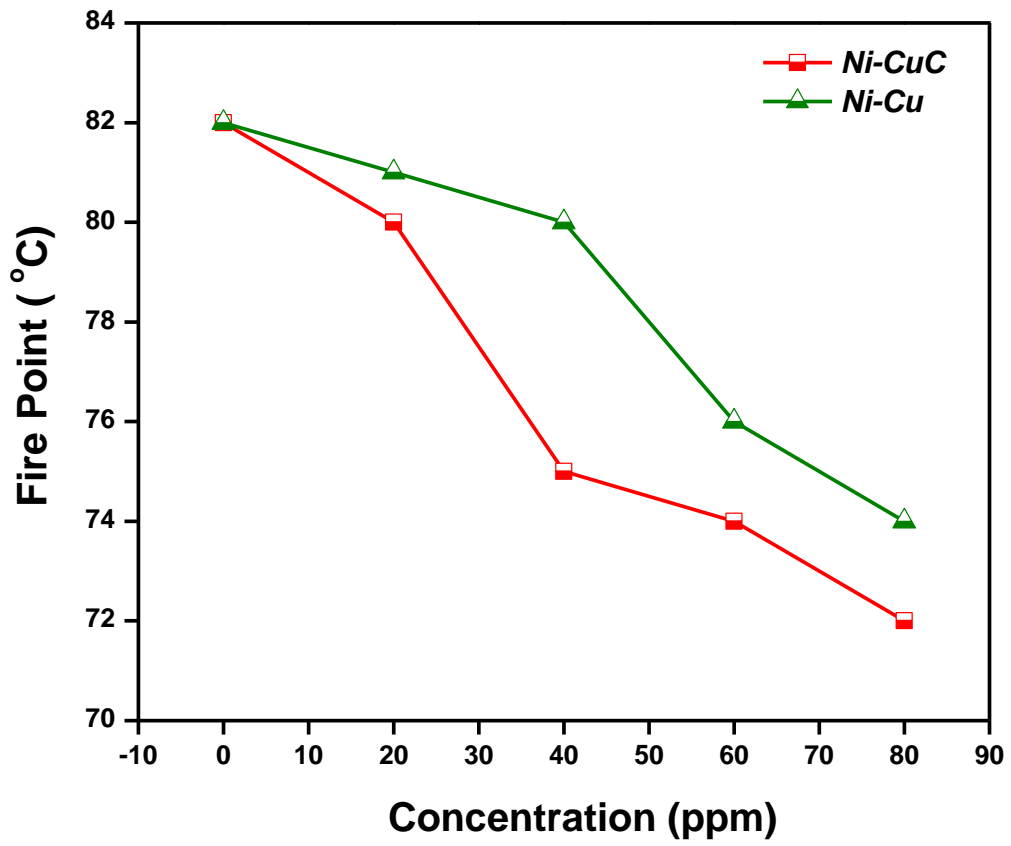


**Fig. 6.** Effect of Ni-Cu and Ni-CuC on onto the fuel fire point of diesel.

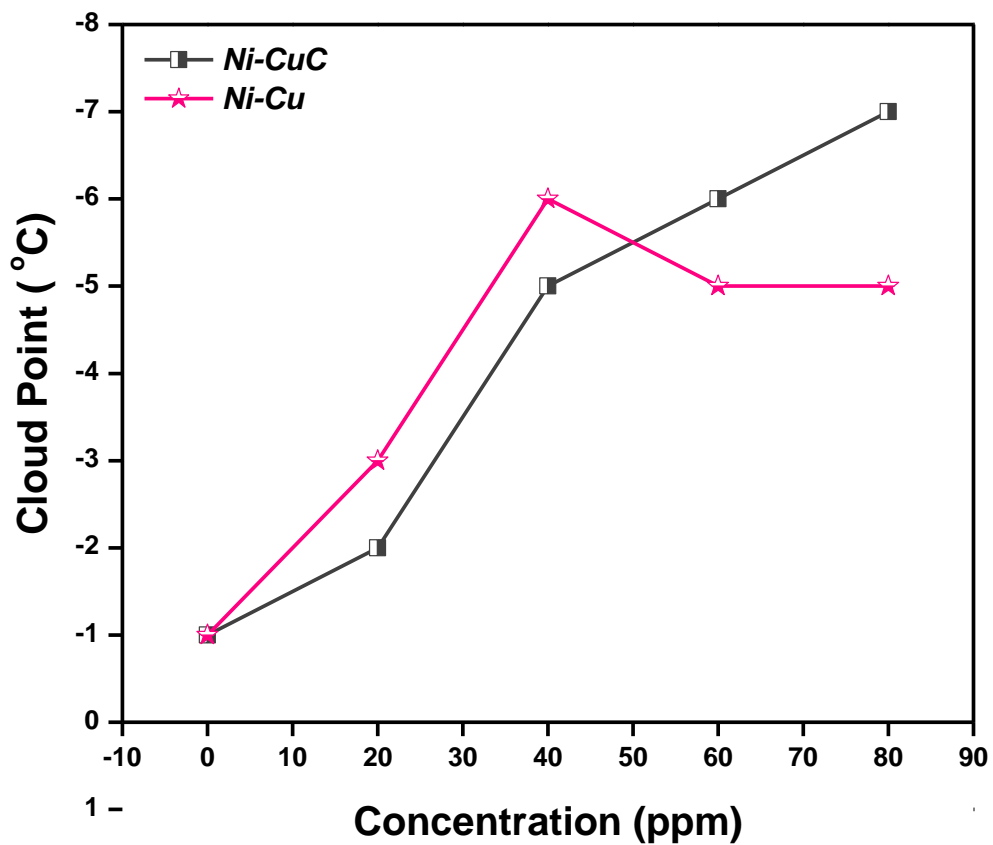


**Fig. 7.** Effect of Ni-Cu and Ni-CuC on cloud point of diesel.

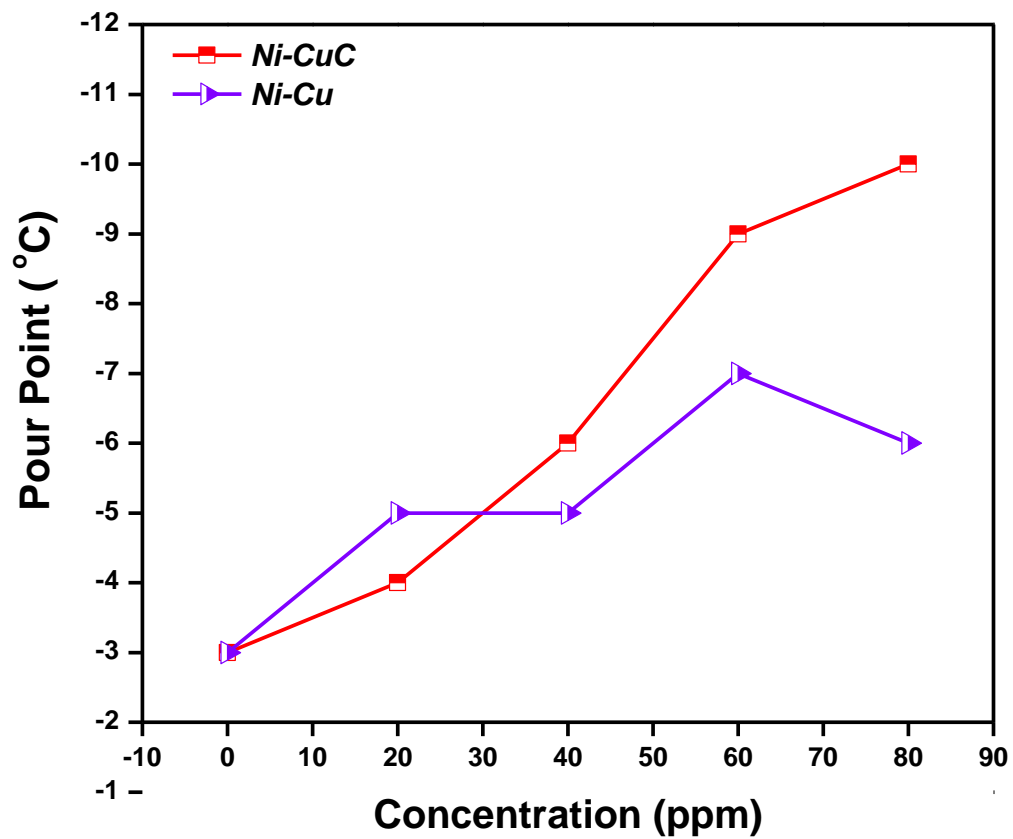


**Fig. 8.** Effect of Ni-Cu and Ni-CuC on pour point of diesel.

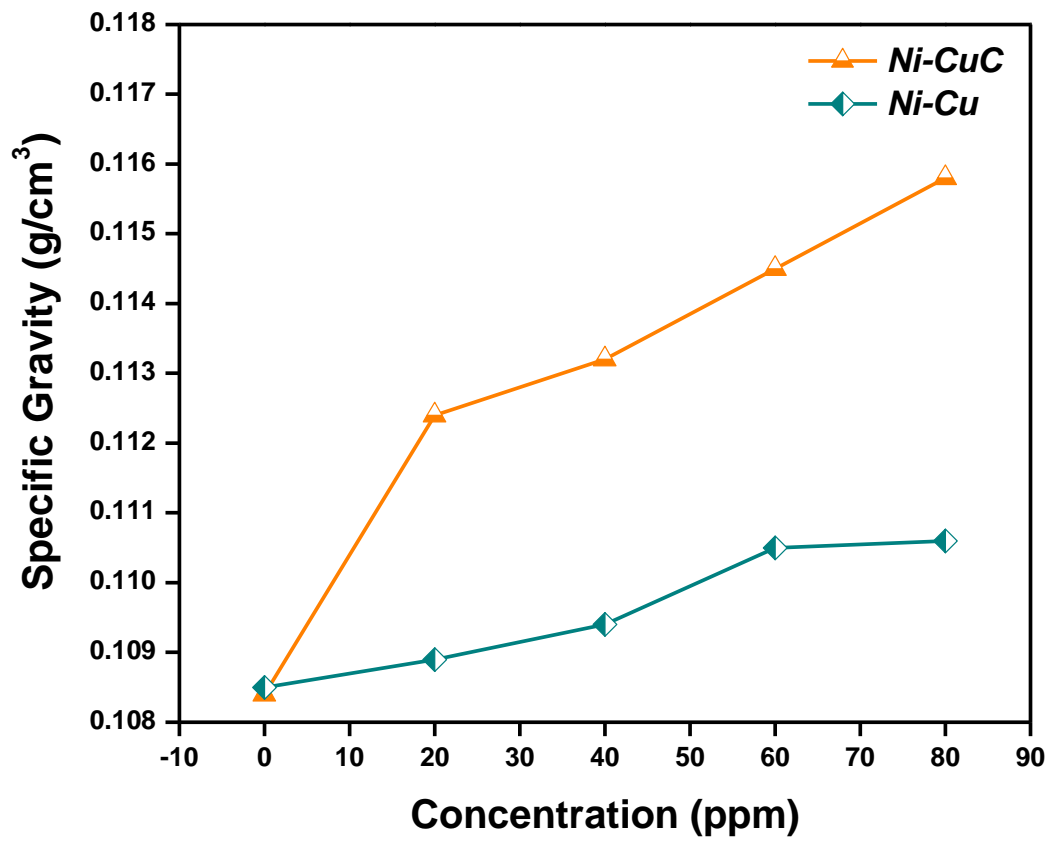
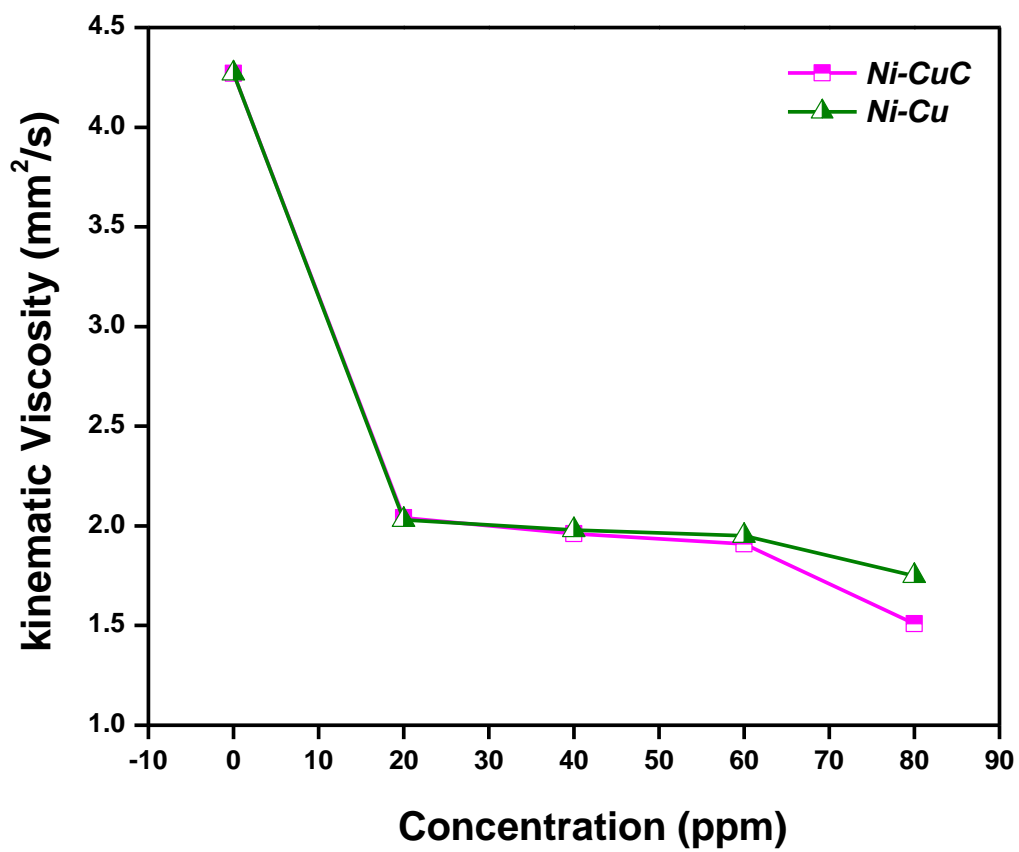
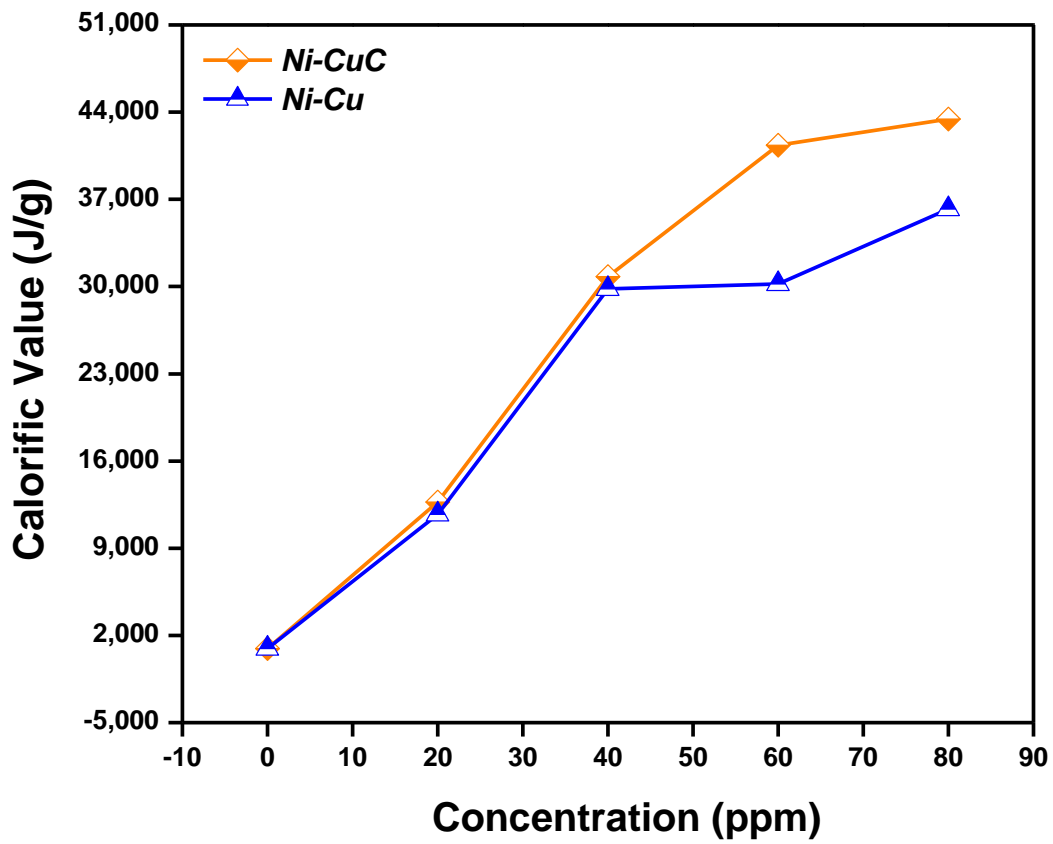


Fig. 9. Effect of Ni-Cu and Ni-CuC on the specific gravity of diesel.



**Fig. 10.** Effect of Ni-Cu and Ni-CuC on kinematic viscosity of diesel.





**Fig. 11.** Effect of Ni-Cu and Ni-CuC on the calorific value of diesel.